Journal of Undergraduate Research **4**, 1 (2010)

Microfluidic Bandage for Localized Oxygen-Enhanced Wound Healing

Z.H. Merchant
Department of Bioengineering, University of Pennsylvania, Philadelphia, PA 19104

J.F. Lo and D.T. Eddington
Department of Bioengineering, University of Illinois at Chicago, Chicago, IL 60607

An oxygen-enhanced, microfluidic bandage was fabricated out of polydimethlysiloxane (PDMS) and contains a 100 μm thick gas-permeable membrane that allows rapid diffusion of oxygen directly to the wound bed. The microfluidic bandage was characterized by measuring the effect of modulating oxygen concentrations, calculating the degree of localization in oxygen delivery when subjected to a non-planar platform, and determining the extent of oxygen penetration below the tissue surface. The concentration of the diffused oxygen (0.02 ± 0.73 to $99.2 \pm 4.46\%$) was shown to rapidly equilibrate ($\sim$30 seconds) to the modulating input oxygen concentration (0 to 100%). The device also maintained localized oxygen delivery to a specified area when a non-planar irregularity was introduced. Finally, the extent of oxygen penetration was found to decrease as the thickness of tissue increased (>75% at 0.8 mm thick). These experiments demonstrate that this microfluidic bandage can be a viable tool for oxygen-enhanced wound healing.

Introduction

Clinical evidence has demonstrated that adequate oxygenation is important in the process of wound healing.[1–5] In the linear phase progression of acute wounds, oxygen has importance in the inflammation, cell migration and proliferation, and tissue remodeling phases.[6] In the inflammation phase, oxygen is converted to Reactive Oxidative Species (ROS), which is a key step in the wound healing pathway at low concentrations and is required for bactericidal activity.[3] Topically applied oxygen has also been shown to induce the production of Vascular Endothelial Growth Factor (VEGF), which accelerates the angiogenesis of the cell migration and proliferation phase.[7] During the tissue remodeling phase, oxygen induces collagen deposition, important for regeneration of the extra-cellular matrix and maintenance of the tensile strength of skin.[6] Oxygen may also trigger the differentiation of fibroblasts into myofibroblasts - cells which are mechanistically similar to smooth muscle cells and are responsible for wound area contraction.[6]

Current oxygen-enhanced wound healing techniques include the Hyperbaric Oxygen Therapy (HBOT) and the Topical Oxygen Therapy (TPOT).[8] HBOT involves placement of the patient in a sealed chamber pressurized to 2-3 atm of 100% O_2.[8] However, one pitfall of HBOT includes subjection of the patient to high atmospheric pressure in a small, enclosed space - conditions that may result in extreme discomfort and claustrophobia. Another problem is the high level of oxygen inhaled can cause neurotoxic conditions and oxidative damage in non-wounded tissues.[5] One solution to HBOT is TPOT, which is the direct topical application of oxygen onto the wound. TPOT is generally applied at 1 atm of 100% O_2 for 1-2 hours a day.[5] Benefits of TPOT include localized delivery of oxygen, prevention of oxygen toxicity, and a more open and comfortable environment than can be found in HBOT.[5] However, current TPOT techniques are still quite expensive and are not portable. In order for future oxygen-enhanced devices to be effective, they must be portable to allow treatment at home, be localized to the wound site, be inexpensive, have no risk of multi-organ oxygen toxicity, allow moisture retention, and allow for rapid diffusion of oxygen through the tissue.[5]

To meet these criteria, a microfluidic bandage was developed to diffuse oxygen directly to the wound. The device was fabricated for a three-year mouse study to measure the effect of oxygen on the rate of wound healing. The device, shown in Figure 1, was fabricated from polydimethylsiloxane (PDMS) and consists of two oxygen-filled chambers 10.0 mm in diameter with microfluidic channels 300 μm wide. The bandage is designed to be connected to medical grade oxygen tanks and permits oxygen to flow into the device. Under each chamber is a 100 μm thick PDMS membrane that allows for rapid diffusion of oxygen from the chamber to the wound, moisture retention, and a degree of elasticity to accommodate any irregularities and unevenness of the skin.

In the characterization of this device, three experiments were performed to understand the effect of modulating oxygen concentration, the extent of localization of oxygen delivery, and the extent of oxygen penetration into the tissue.

Materials and Methods

Fabrication of Microfluidic Bandage

The oxygen-enhanced microfluidic bandage was fabricated using standard soft-lithography techniques in a four part process: microfluidic chamber and channels, PDMS membrane for gas-diffusion, chamber cap, and ports as seen in Figure 1(b).

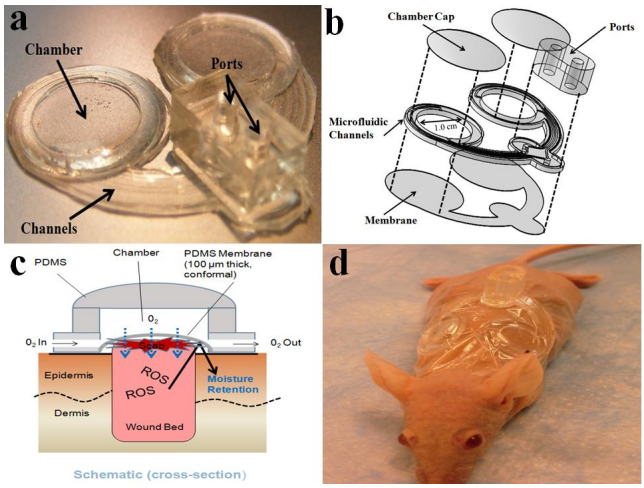

FIG. 1: a) The chamber and the ports are indicated on a microfluidic, oxygen-enhanced bandage. The device was fabricated from polydimethylsiloxane (PDMS), which is a moldable, biocompatible, and gas-permeable material; b) an exploded model of the device showing all of the parts; c) a cross-section schematic of the one chamber positioned over the wound; Oxygen is shown to enter the chamber and diffuse onto the wound through the 100 μm thick PDMS membrane; d) the microfluidic device attached to a hairless mouse (strain STZ) for a three-year animal study to analyze the effect of this oxygen-enhanced bandage on the rate of wound healing.

The microfluidic channels and chamber was designed using AutoCAD and printed onto a 16k *dpi* photomask. SU-8-2150 photoresist (MicroChem, Newton, MA) was spun to 100 μm thick according to the manufacturer's protocol. The SU was then placed under the photomask and exposed to ultraviolet light, causing the SU8 to selectively crosslink only at the uncovered areas. After exposure baking and further crosslinking of exposed area, the uncrosslinked areas were removed with SU-8 developer (MicroChem, Newton, MA), leaving a positive master mold. Once the master was fabricated, premixed 10:1 ratio of PDMS prepolymer and curing agent was poured onto the master until the PDMS was 1.0 mm thick. The PDMS mixture was cured for 2 hours at 90°C. Holes were then made for the chamber and ports.

The 100 μm thick gas-permeable PDMS membrane was made by spinning PDMS on a silicon wafer using a precision spinner. The wafer was spun at 500 RPM for 10 seconds to spread the PDMS droplet, and then at 800RPM for 30 seconds. The membrane was cured for 5 minutes at 85°C.

The chamber cap was fabricated by dropping ∼150 μl of PDMS onto a silicon wafer heated to 120°C and then removing the PDMS once cured. Once all parts of the device were fabricated, every part surface was treated for 30 seconds under a corona plasma device (STP, Inc) prior to bonding. The completed device was baked at 100°C for 1-2 hours to further strengthen the bonding. ground.

Leakage Test

To locate any leaks in the bandage, the device was submerged in water, and a gas line was connected to the ports. Any bubbles that formed indicated a leaky device to be discarded.

Oxygen Concentration Validation

An oxygen-sensing chip coated with a ruthenium fluorescent dye (FOXY slide, OceanOptics) was used to quantify the oxygen concentration that diffused through the gas-permeable PDMS membrane. Because the fluorescence of the ruthenium dye is quenched in the presence of oxygen, the concentration of oxygen can be calculated by measuring the fluorescent intensity. By capturing a time-lapse image of the fluorescence using fluorescence equipped inverted Olympus IX71 microscope and MetaMorph software package, the change in oxygen concentration was followed over time. The fluorescent intensities were empirically fit to a Stern-Volmer model, which was used to convert the intensities to oxygen concentration.[9] All images were acquired at 38°C (physiological temperature) using a FOXY-compatible fluorescent filter with excitation wavelength of 475 nm and emission wavelength of 600 nm.

Characterization: Modulation of Oxygen Concentrations

Equilibration of the microfluidic bandage to 0% oxygen concentration was achieved by pumping a mixture of 5% CO_2 and 95% N_2 into the device for 10 minutes. After 0% equilibration, the input concentration was switched to 100% O_2, and the concentration of the diffused oxygen through the 100 μm thick PDMS membrane was measured. This process was repeated, measuring the change in oxygen concentration after switching the input concentration from 0 to 10.5, 21, and 60.5% O_2. This experiment was repeated at each input concentration on three different devices.

Characterization: Localization of Oxygen Delivery in Conformal and Non-Conformal Devices

This experiment was conducted to demonstrate the improved sealing of the device design. Because our chamber has a large width to height ratio, standard engineering design suggests that the chamber should have interior pillars to prevent collapse. However, with the pillars, the device is unable to accommodate the uneven topology

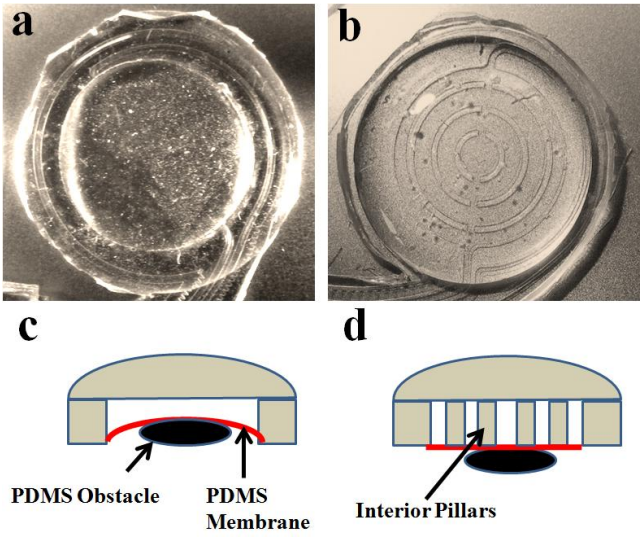

FIG. 2: a) The conformal microfluidic lacks interior pillars to support the chamber; b) the non-comformal microfluidic bandage was fabricated with interior pillars to prevent collapse; c) a schematic cross-section side view of the conformal chamber. The PDMS membrane is shown to wrap around the PDMS obstacle; d) a side view of the non-conformal chamber. The interior pillars prevent the PDMS membrane to conform around the obstacle.

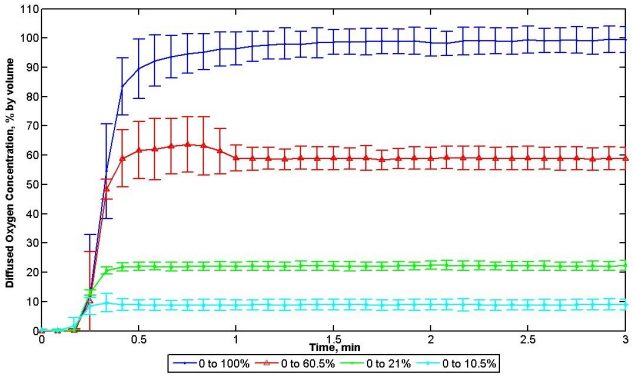

FIG. 3: A range of gas concentrations were rapidly diffused (<30 s equilibrium) through the PDMS membrane. Modulation of oxygen was achieved by first equilibrating the device to 0% O_2 (5% CO_2, 95% N_2) and then switching the input concentration to 10.5, 21, 60.5, or 100% O_2.

Input Concentration (% O_2)	**Diffused Concentration at Equilibrium(average ± standard deviation, % O_2)**
10.5	8.88 ± 1.81
21.0	22.2 ± 1.50
60.5	58.9 ± 3.89
100	99.2 ± 4.46

TABLE I: Modulation of Oxygen Concentrations

that is common to a healing wound, causing delocalization of the oxygen delivery. To measure the extent of oxygen localization with and without the pillars, two devices were fabricated for this experiment: one in which the PDMS membrane is attached only to the circumference of the chamber (Figures 2(a), 2(c)), and one in which the flexibility of the PDMS membrane is impeded by pillars in the chamber (Figures 2(b), 2(d)). The chamber of each type of device was placed on a custom made disk of PDMS 8 mm in diameter and 0.5 mm thick. Each type of device was equilibrated to 0% O_2 and then the input concentration was switched to 100% O_2. The diffused oxygen concentration was measured. Three trials were conducted for each type of device.

Characterization: Extent of Oxygen Penetration

Oxygen penetration was measured by calculating the concentration of oxygen after the oxygen diffused through a PDMS membrane and a phantom tissue. The phantom tissue, consisting of 3% agar (Fisher Scientific), was sliced to a desired thicknesses ranging from 0.2-1.0 mm. The chamber was placed directly on top of a sliced phantom tissue of selected thickness. The microfluidic bandage was equilibrated to 0% O_2, and then the input concentration was switched to 100% O_2. At each thickness, three trials were conducted using the same device.

Results

Characterization: Modulation of Oxygen Concentrations

The change concentration of diffused oxygen through the PDMS membrane was recorded at each switch of the input concentration from 0% to, 10.5, 21, 60.5, and 100% O_2 as shown in Figure 3. The average diffused concentration at equilibrium with 0% input was 0.02 ± 0.73%. Equilibration of the diffused oxygen concentrations are achieved within 30 seconds. For each concentration, the diffused output oxygen concentration approximately equilibrated to its respective input concentration (Table I).

Characterization: Localization of Oxygen Delivery in Conformal and Non-Conformal Devices

The change in the diffused oxygen concentration under the chamber and exterior to the device was mapped in Figures 4(a) and 4(b) for the conformal and non-conformal devices, respectively, when they were placed over the PDMS obstacle. For the conformal device, the

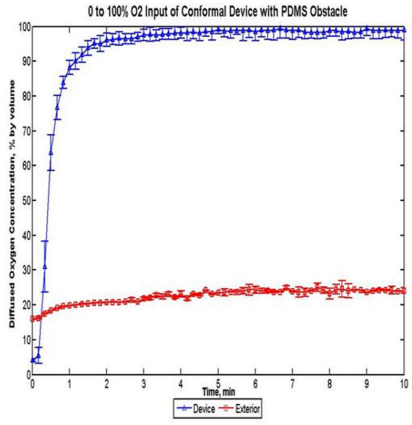

(a)

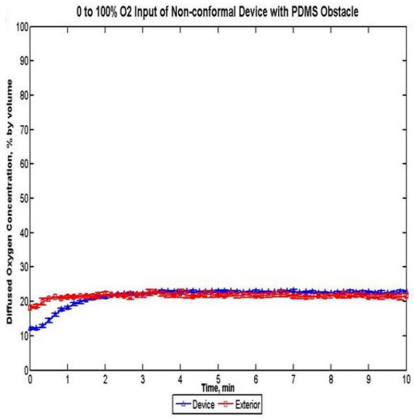

(b)

FIG. 4: a) The diffused concentration in the conformal device was measured when the input concentration was changed from 0 to 100% O_2. Localization was achieved by providing 100% O_2 only to directly under the chamber; b) a catastrophic failure is seen in the non-conformal device, as the diffused oxygen concentration did not rise significantly above ambient at 100% O_2 input.

diffused oxygen concentration rapidly changed from 0 to 99.5 ± 4.40% O_2 (average concentration at equilibrium), while the oxygen concentration exterior to the device was maintained at ambient oxygen concentrations (∼21% O_2). In the non-conformal bandage, the average concentration achieved at equilibrium with 100% O_2 input was 22.61 ± 0.44% O_2 with exterior normoxic conditions.

Characterization: Extent of Oxygen Penetration

The penetration of oxygen at 1, 3, and 5 minutes of 100% O_2 input through increasing thicknesses of 3% agar is displayed in Figure 5. In general, as the depth of the phantom tissue increased, the oxygen concentration through that depth decreased. At 5 minutes of 100%

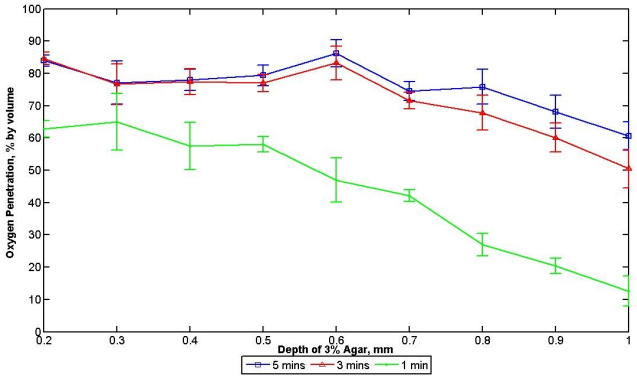

FIG. 5: Penetration of oxygen at varying depths of 3% agar phantom tissue at 1, 3, and 5 minutes after input O_2 was changed from 0 to 100%.

O_2 input, concentration at 0.8mm thickness was 75.8 ± 5.38% O_2.

Discussion and Conclusions

Characterization: Modulation of Oxygen Concentrations

The microfluidic bandage is able to precisely deliver oxygen directly to the wound, with concentrations ranging from 0.02 ± 0.73 to 99.5 ± 4.40%. Equilibration for all input concentrations tested was achieved within 30 seconds. Because of this high degree of precision, the user of the device is able to provide oxygen to the wound at any desired concentration. The short equilibration time allows the user to quickly cycle between two or more concentrations in any protocol that may require hypoxic, hyperoxic, or intermittent hypoxic conditions.

Characterization: Localization of Oxygen Delivery in Conformal and Non-Conformal Devices

The conformal device without the interior pillars had a high degree of localization and sealing - this device will be able to conform around non-planar irregularities of the skin, allowing delivery of 100% O_2 only to the wound under the chamber, while leaving the part of the skin exterior to the chamber at ambient oxygen concentrations. The non-conformal device with the interior pillars did not deliver the oxygen locally, with the diffused oxygen concentration barely reaching above 21%. It was expected that mixing of the diffused 100% with ambient 21% at the exterior of the device would yield the equilibration of diffused oxygen concentration at about 60%. However, it may be deduced that the interior pillars in the non-conformal device caused so much inelasticity that the PDMS obstacle may have blocked diffusion of oxygen to

the sensor. Thus, the removal of pillars in the conformal bandage is critical for non-planar features such as scabbing and scarring during wound healing.

Characterization: Extent of Oxygen Penetration

As expected, the diffused oxygen concentration decreased as the thickness of the phantom tissue increased. However, even after 5 minutes of 100% O_2 input, the concentration of 0.8 *mm* was above 75%. This is important because 0.8 *mm* lies within the range of thickness of the human epidermis (0.4-1.5 *mm*).[10] Measuring the extent of oxygen penetration is necessary because it allows the user of the oxygen-enhanced bandage to not only control the oxygen concentration delivered to the surface of the wound, but also the oxygen concentration delivered to the epidermis and dermis. Thus, this experiment demonstrates that consistently high concentrations of oxygen can be distributed beneath the surface of the skin when 100% O_2 is delivered to the surface. Note that while the trend seems to be linear in the range of thicknesses tested, we might expect that at greater thicknesses, an exponential decay should be more apparent, following an expected diffusion-based trend.

Future Work

This oxygen enhanced micro-fluidic bandage will be used in a three-year mouse study to assess the effect of oxygen delivered by this device on the rate of wound healing. Specifically, we will measure the change in the rate of wound closure with bandage under hypoxic and hyperoxic conditions. We will also test the rate of collagen deposition and the levels of VEGF with the device.

Acknowledgments

This project was supported financially by the National Science Foundation and the Department of Defense, EEC-NSF Grant # 0755115. The experiments and analysis were conducted at the University of Illinois at Chicago in the Biological Microsystems Laboratory. The author (Zameer Merchant) would like to thank Dr. Christos Takoudis and Dr. Greg Jursich for their leadership and guidance in this project.

[1] R. Fries, W. Wallace, S. Roy, P. Kuppusamy, V. Bergdall, G. Gordillo, W. Melvin, and C. Sen, Mutation Research-Fundamental and Molecular Mechanisms of Mutagenesis **579**, 172 (2005), ISSN 0027-5107.

[2] S. C. Davis, A. L. Cazzaniga, C. Ricotti, P. Zalesky, L.-C. Hsu, J. Creech, W. H. Eaglstein, and P. M. Mertz, Archives of Dermatology **143**, 1252 (2007), ISSN 0003-987X.

[3] G. Gordillo and C. Sen, American Journal of Surgery **186**, 259 (2003), ISSN 0002-9610.

[4] H. Said, J. Hijjawi, N. Roy, J. Mogford, and T. Mustoe, Archives of Surgery **140**, 998 (2005), ISSN 0004-0010.

[5] L. Kalliainen, G. Gayle, R. Schlanger, and C. Sen, Pathophysiology (2003).

[6] M. Franz, in *Current Diagnosis & Treatment Surgery* (2006).

[7] G. M. Gordillo, S. Roy, S. Khanna, R. Schlanger, S. Khandelwal, G. Phillips, and C. K. Sen, Clinical and Experimental Pharmacology and Physiology **35**, 957 (2008), ISSN 0305-1870.

[8] C. K. Sen, Wound Repair and Regeneration **17**, 1 (2009), ISSN 1067-1927.

[9] A. Vollmer, R. Probstein, R. Gilbert, and T. Thorsen, Lab on a Chip **5**, 1059 (2005), ISSN 1473-0197.

[10] D. H. Chu, in *Fitzpatrick's Dermatology in General Medicine 7* (2008).